CrossMark
click for updates

methods

Quantitative structural characterization of phosphatidylinositol phosphates from biological samples[S]

Su Hee Kim,* Ha Eun Song,* Su Jung Kim,* Dong Cheol Woo,*,† Suhwan Chang,§ Woo Gyun Choi, Mi Jeong Kim,** Sung Hoon Back,** and Hyun Ju Yoo[1,*,†]**

Biomedical Research Center,* Department of Convergence Medicine,† and Division of Biomedical Sciences,§ Asan Institute for Life Sciences, Asan Medical Center, University of Ulsan College of Medicine, Seoul 05505, Republic of Korea; and School of Biological Sciences,** University of Ulsan, Ulsan 44610, Republic of Korea

Abstract The aspects of cellular metabolism controlled by phosphatidylinositol phosphates (PtdInsPs) have been broadly expanded, and these phospholipids have drawn tremendous attention as pleiotropic signaling molecules. PtdInsPs analysis using LC/MS/MS has remained challenging due to the strong hydrophilicity of these lipids. Multiple reaction monitoring (MRM) or a neutral loss scan has been performed to quantitatively measure PtdInsPs after chemical derivatization on the phosphate groups of inositol moieties. Only predefined PtdInsPs can be measured in MRM mode, and fatty acyl compositions of *sn*-1 and *sn*-2 positions of PtdInsPs cannot be obtained from a neutral loss scan. In our present study, we developed a simple LC/MS/MS method for structural identification of *sn*-1 and *sn*-2 fatty acids of PtdInsPs and their relative quantitation. Precursor ion scans of *sn*-1 monoacylglycerols (MAGs) of PtdInsPs provided structural information about the lipids, and ammonium adduction enhanced signal intensities of PtdInsPs. The relative amount of observed PtdInsPs in biological samples could be compared using chromatographic peak areas from the neutral loss scans. Using precursor ion scans of *sn*-1 MAG and neutral loss scans of headgroups, major PtdInsPs in cells and tissues were successfully identified with structural information of *sn*-1 and *sn*-2 fatty acids, and their relative amounts in different samples were compared.—Kim, S. H., H. E. Song, S. J. Kim, D. C. Woo, S. Chang, W. G. Choi, M. J. Kim, S. H. Back, and H. J. Yoo. **Quantitative structural characterization of phosphatidylinositol phosphates from biological samples.** ***J. Lipid Res.*** **2017.** 58: **469–478.**

Supplementary key words phosphoinositides • fatty acids • lipidomics • high-performance liquid chromatography • tandem mass spectrometry

Phosphatidylinositol phosphates (PtdInsPs), a type of cellular phospholipids, play an important role in signal transduction, membrane dynamics, and cell proliferation (1–4). The aspects of cellular metabolism controlled by PtdInsPs have been broadly expanded, and PtdInsPs have drawn tremendous attention as pleiotropic signaling molecules for eukaryotic cells in a wide range of biomedical research (5, 6). This class of phospholipids regulates biology by controlling vesicular trafficking and also by modulating lipid distribution and metabolism via close interaction with proteins (7–9). Dysregulation of PtdInsPs is known to be involved in various human diseases, such as cancer, obesity, and diabetes (10, 11). For example, the relationship between phosphatidylinositol 3-kinase (PI3K) and oncogenic receptor tyrosine kinases puts an emphasis on the role of PtdInsPs in cancer biology. PtdInsPs promote cell proliferation and prevent apoptosis; thus, they are known as representative oncogenic lipids (10).

PtdInsPs are generated metabolically via phosphorylation on the hydroxyl groups of the inositol sugar of phosphatidylinositol (PtdIns). This phosphorylation is regulated by the enzymatic action of several kinases and phosphatases. In general, monophosphorylation of PtdIns occurs in endomembranes such as the Golgi, and di- or triphosphorylation occurs mainly in plasma membranes (10). PtdInsPs exist in various cells and tissues, and their amount shows significant variation (12, 13). PtdIns and PtdInsPs are low-abundance lipid classes consisting of 10%–20% of total cellular phospholipids. Phosphatidylinositol bis- ($PtdInsP_2$) or triphosphates ($PtdInsP_3$) constitute less than 1% of the total of PtdIns and PtdInsPs (14, 15). The amount of $PtdInsP_3$ contributes 2%–5% of $PtdInsP_2$ or less than 0.25% of the inositol lipids in eukaryotic cell membranes (10, 16). Observing $PtdInsP_3$ in biological samples is difficult, even upon stimulation (17).

This work was supported by a grant (W14-540) from Asan Institute for Life Sciences, Asan Medical Center, Seoul, and by the Basic Science Research Program through the National Research Foundation of Korea funded by the Ministry of Science, ICT and Future Planning (2014R1A1A1003608, 2014R1A6A1030318), Republic of Korea.

Manuscript received 12 June 2016 and in revised form 6 December 2016.

Published, JLR Papers in Press, December 9, 2016
DOI 10.1194/jlr.D069989

Abbreviations: CID, collision-induced dissociation; DAG, diacylglycerol; EIC, extracted ion chromatogram; MAG, monoacylglycerol; PtdIns, phosphatidylinositol; $PtdInsP_2$, phosphatidylinositol bisphosphate; $PtdInsP_3$, phosphatidylinositol triphosphate; PtdInsP, phosphatidylinositol phosphate.

[1]To whom correspondence should be addressed.
e-mail: yoohyunju@amc.seoul.kr

[S] The online version of this article (available at http://www.jlr.org) contains a supplement.

Copyright © 2017 by the American Society for Biochemistry and Molecular Biology, Inc.

This article is available online at http://www.jlr.org

This is an Open Access article under the CC BY license.

PtdInsPs have been deacylated and analyzed by measuring ^{32}P-labeled inositides or ^{3}H-myo-inositol using HPLC (18–20). TLC has been conventionally used for the analysis of phospholipids and has been applied to analyze isomers of PtdInsPs (21, 22). A TLC analysis is relatively nonspecific, and lipids extracted from a TLC plate have been further analyzed with GC or GC/MS (23). These methods using radiolabeling with ^{32}P or a TLC separation are very laborious and have limited applications. Mass spectrometric detection of phospholipids has been performed in a positive or negative ion mode. Collision-induced dissociation (CID) is the most commonly used tandem mass spectrometric strategy. CID in a positive ion mode provides structural information about the polar headgroups of phospholipids. Haag et al. (17) determined PtdInsPs from human T cells before and after stimulation in a positive ion mode, through diacylglycerol (DAG) ions resulting from neutral loss of the headgroup from PtdInsPs. On the other hand, the fatty acid composition attached at the *sn*-1 or *sn*-2 position of the phospholipids was obtained from negative ion mode CID. Several research groups have performed structural characterization of PtdInsPs using CID in negative ion mode, and determined fatty acyl compositions using the neutral loss of free fatty acid substituents or corresponding ketens (13, 16, 24, 25). Thus, mass spectrometric analysis from both positive and negative ion modes should be required for complete structural elucidation of PtdInsPs. However, neutral loss scans of free fatty acid substituents may not be suitable for routine analysis of PtdInsPs due to the lack of sensitivity in negative ion mode, compared with those in positive ion mode. An ELISA has been used to analyze PtdInsP, PtdInsP$_2$, or PtdInsP$_3$. However, different types of ELISA kits are necessary for each class of PtdInsPs species, and the fatty acyl composition of PtdInsPs cannot be identified by this approach (26, 27).

Recently, LC/MS or LC/MS/MS has been widely used for analysis of various phospholipids including PtdInsPs (28–30). LC/MS/MS is able to detect intact phospholipids without deacylation or chemical derivatization and provides valuable structural information for the identification of phospholipids. Phosphate groups on the inositol moiety render distinct chemical properties on PtdInsPs compared with other types of phospholipids. Observing positively charged PtdInsPs during a mass spectrometric analysis is difficult due to the acidic nature of phosphates. Thus, structural identifications using a tandem mass spectrometric analysis for PtdInsPs have been published using the deprotonated forms (13, 16, 25, 30). Ion suppression during the electrospray ionization process could be more problematic for PtdInsPs because they are low abundance lipids in biological samples. MS combined with an LC separation module could be a suitable method for analysis of PtdInsPs from various biological samples to discriminate isomers and to overcome ion suppression. Reverse-phase liquid chromatography (RPLC) separation has generally resulted in poor performance due to the high polarity of the phosphate groups on PtdInsPs. Ogiso et al. (30) reported successful separation of deprotonated PtdInsPs using C8 columns under strong alkaline conditions. In addition, a normal-phase column has been tried to separate highly polar PtdInsPs (28, 31).

TMS-diazomethane has been used to methylate carboxylic acids or phosphates (14, 32, 33). Wasslen et al. (33) showed that trimethylsilylation enhanced the ionization efficiencies and sensitivities of glycerophospholipids and provided clearer fragmentation patterns than unmodified glycerophospholipids. Polar lipids, including glycerophospholipids, showed increased signal enhancement due to better ionization efficiencies after methylation. In addition, methylation of glycerophospholipids has resulted in better chromatographic peak shapes and resolution, compared with those of nonmethylated molecular species (34). Methylation of the phosphate groups of the inositol moiety could enhance an RPLC separation and ionization efficiencies of PtdInsPs, as well as prevent nonspecific binding of PtdInsPs within LC/MS systems. Thus, methylation of phosphate groups should be especially beneficial for the analysis of highly phosphorylated PtdInsP$_2$ and PtdInsP$_3$ (35), which typically exist in very low levels in biological samples. PtdInsPs from cells have been measured using a neutral loss scan upon headgroup fragmentation in the positive ion mode after derivatization with TMS-diazomethane (14). Clark et al. (35) successfully quantified PtdInsP$_3$ along with other PtdInsPs from stimulated cells and liver tissues using LC/MS/MS after TMS-diazomethane derivatization. They performed MS^2 analysis for individual PtdInsPs to get the information of the *sn*-1 and *sn*-2 fatty acyl compositions of the observed PtdInsPs.

Methylation of PtdInsPs successfully enables detection of PtdInsPs in biological extracts using LC/MS/MS but was at the limits of detection for quantitation of PtdInsP$_3$. We have determined whether detection limits can be improved by using ammonium adduction. This would be especially crucial to profile PtdInsPs using neutral loss scans to search for more PtdInsPs in biological extracts because the sensitivity in scan mode is lower than that in nonscanning technique such as multiple reaction monitoring. In addition, it would be advantageous for precursor ion scans of *sn*-1 monoacylglycerol (MAG) in positive ion mode to get fatty acid compositions at *sn*-1 and *sn*-2 positions of PtdInsPs. In this study, the combined strategy of precursor ion scans of *sn*-1 MAG and neutral loss scans of headgroups was successfully applied to compare the relative amounts of PtdInsPs in biological samples. Hepatocytes and mice livers were used to explore the changes of PtdInsPs after insulin stimulation.

MATERIALS AND METHODS

Materials and sample preparation

PtdInsPs were purchased from Avanti Polar Lipids (Alabaster, AL). The PtdInsPs were the following: 17:0/20:4 PtdIns (17:0/20:4 PtdIns), 18:0/20:4 PtdIns (18:0/20:4 PtdIns), 17:0/20:4 PtdIns(3)P (17:0/20:4 PtdInsP), 18:1/18:1 PtdIns(3)P (18:1/18:1 PtdInsP),

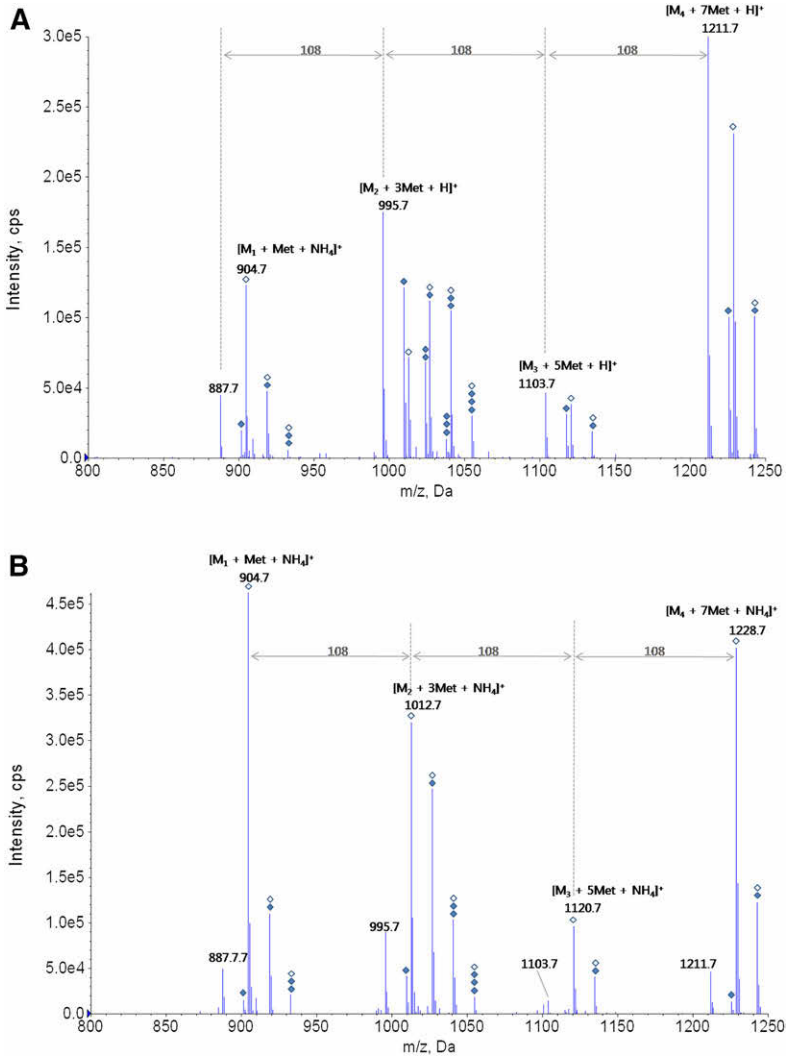

Fig. 1. Mass spectra of permethylated PtdInsPs (M_1 = 17:0/20:4 PtdIns, M_2 = 17:0/20:4 PtdInsP, M_3 = 17:0/20:4 PtdInsP_2, M_4 = 17:0/20:4 PtdInsP_3) when 0.1% formic acid (A) or 5 mM ammonium formate (B) was included in the LC mobile phases. The number of filled diamonds indicates the number of overmethylation to each permethylated PtdInsP, and open diamonds indicate ammonium ion adduction.

17:0/20:4 PtdIns(3,4)P_2 (17:0/20:4 PtdInsP_2), 18:0/20:4 PtdIns(3,4)P_2 (18:0/20:4 PtdInsP_2), 17:0/20:4 PtdIns(3,4,5)P_3 (17:0/20:4 PtdInsP_3), and 18:0/20:4 PtdIns(3,4,5)P_3 (18:0/20:4 PtdInsP_3). All stock solutions were prepared in methanol and stored at −20°C. All solvents and chemicals were purchased from Sigma-Aldrich (St. Louis, MO) or J.T. Bakers (Philipsburg, NJ).

PtdInsPs from biological samples were extracted by using the Folch method with minor modifications (36). Five hundred microliters of $CHCl_3$/methanol/12M HCl (80:40:1, v/v/v) and 100 µl of internal standard solution (10 µM each of 17:0/20:4 PtdInsPs in methanol) were added to approximately a million AML cells or 20–50 mg of mice livers. Samples were homogenized using a TissueLyzer (Qiagen Inc., Valencia, CA), and allowed to stand for 25 min at room temperature to ensure all PtdInsP dissolved in solvents. After centrifugation, the supernatant was collected for the extraction of PtdInsPs. Then, 170 µl of $CHCl_3$ and 340 µl of 0.01 M HCl were added to the supernatant, followed by vigorous vortexing. The bottom organic layer containing the lipids was collected and transferred to a new tube. Another 170 µl of $CHCl_3$ was added to the remaining solution. After vigorous vortexing and centrifugation, the bottom organic layer was collected and added to the previously collected organic layer. The organic layer presumably containing PtdInsPs was dried under vacuum. The dried extract was kept at −20°C prior to chemical derivatization. Standard solutions of PtdInsPs were prepared using the same procedure as described for biological samples. The dried extract was reconstituted in 100 µl methanol, and 20 µl of 2 M TMS-diazomethane in hexane (Sigma-Aldrich) was added. The derivatization reaction was allowed to proceed for 30 min at room temperature, and 3 µl glacial acetic acid was added to the reaction solution. Four hundred fifty microliters $CHCl_3$/methanol/water (8:4:3, v/v/v) was added to the reaction solution, and the solution underwent vigorous vortexing. After centrifugation, the organic layer of the solution was collected and dried under vacuum. The dried extract was reconstituted in 30 µl methanol for the LC/MS/MS analysis.

Cell culture and insulin treatment

The mouse hepatocyte cell line AML12 cells were purchased from the ATCC (Manassas, VA). Cells were maintained in DMEM/F12 (Welgene Inc., Gyeongsan-si, Republic of Korea) supplemented with 10% FBS, dexamethasone (100 nM) and 1× insulin-transferrin-selenium-pyruvate supplement solution (Welgene Inc.). Cells were cultured in DMEM/F12 without any supplements overnight before insulin treatment. For experiments, the cells were incubated in DMEM/F12 with PBS or insulin (100 ng/ml or 1,000 ng/ml) for 20 min. After the incubation, the cells were immediately collected and washed with PBS. The cells were lysed with cold methanol and vigorous vortexing, then kept at –80°C until processing.

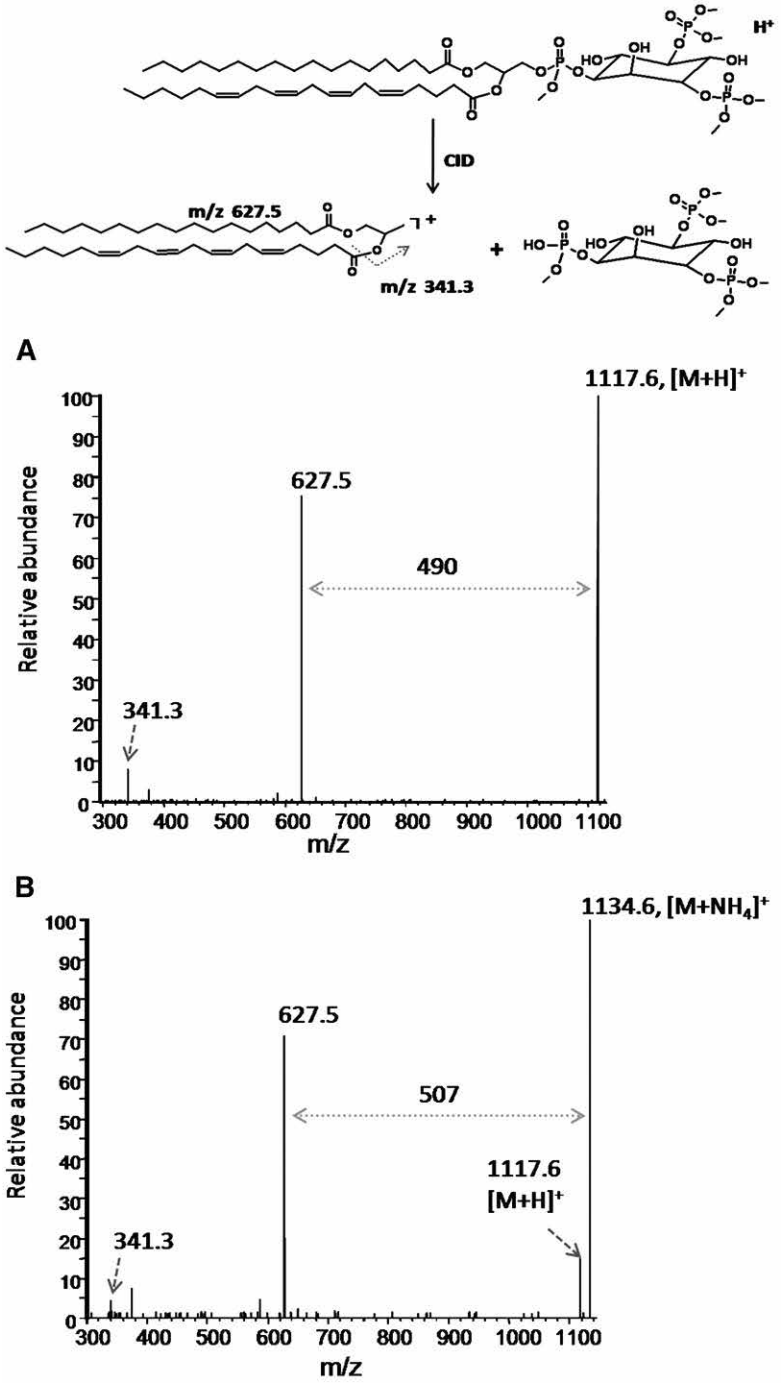

Fig. 2. CID spectra of $[M + H]^+$ (A) and $[M + NH_4]^+$ (B) for M = 18:0/20:4 $PtdInsP_2$ + 5Met. Collision energies were 30 V.

Insulin-treated mice

Mice were housed at 21°C–23°C with 12 h light and 12 h dark cycles in the Specific Pathogen Free animal facility at the University of Ulsan with free access to water and standard rodent chow. All animal care and procedures were conducted according to the protocols and guidelines approved by the University of Ulsan Animal Care and Use Committee. After anesthesia, female C57BL/6 mice at 8 weeks of age were administered with PBS or insulin (1 U/kg body weight via the vena cava). Five minutes after insulin infusion, the liver was removed and frozen in liquid nitrogen and kept at –80°C until processing.

LC/MS/MS

An LC/MS/MS system equipped with 1290 HPLC (Agilent Technologies, Glostrup, Denmark), Qtrap 5500 (AB Sciex, Framingham, MA), and a reverse-phase column (Pursuit 5 C18 150 × 2.0 mm; Agilent Technologies, Santa Clara, CA) was used. MS was operated in the positive ion mode with turbo ion-spray voltage of 5,500 V, using 20 psi curtain gas, 50 psi nebulizer gas, and 50 psi drying gas at a temperature of 400°C. The LC separation for PtdInsPs used mobile phase A (5 mM ammonium formate-methanol-tetrahydrofuran; 500:200:300) and mobile phase B (5 mM ammonium formate-methanol-tetrahydrofuran; 100:200:700), and proceeded at 200 µl/min and 23°C. The separation gradient was as follows: 5% of B at 0 min, 5% of B for 10 min, 5% to 90% of B for 35 min, 90% of B for 0.1 min, and then 90% to 5% of B for 14.9 min. For comparison, mobile phase A (0.1% formic acid-methanol-tetrahydrofuran; 500:200:300) and mobile phase B (0.1% formic acid-methanol-tetrahydrofuran; 100:200:700) were also used with the same gradient. A neutral

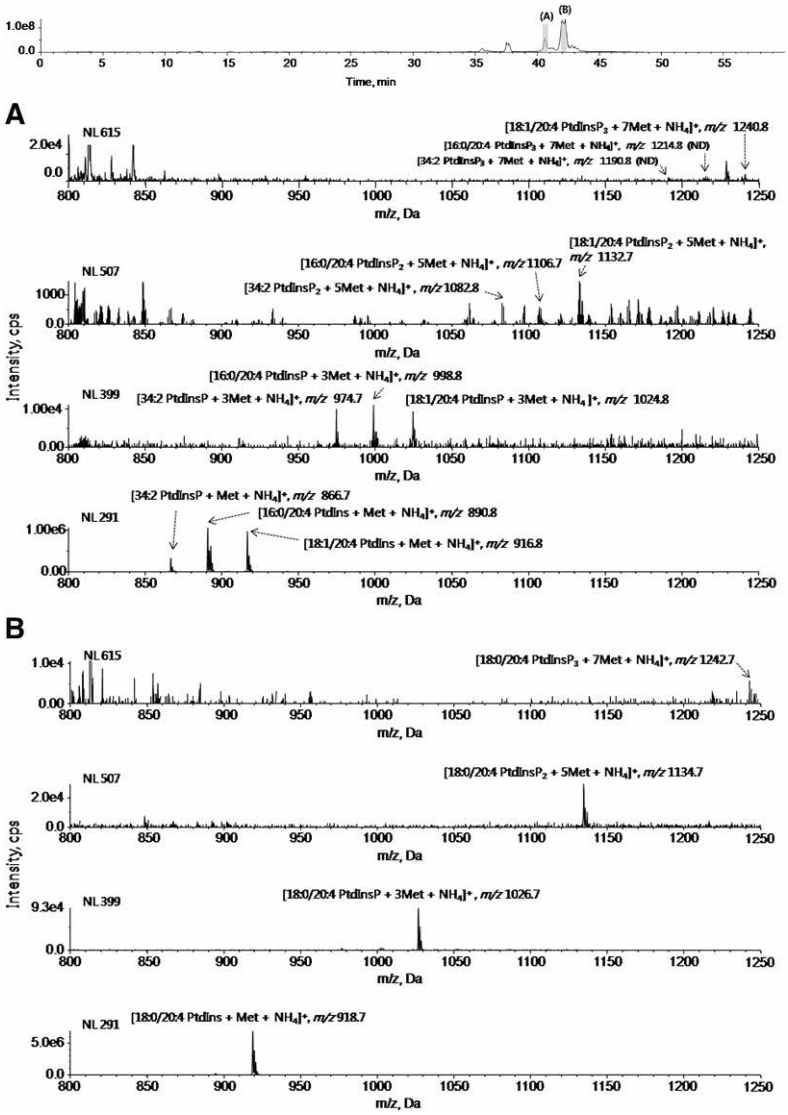

Fig. 3. Mass spectra of neutral loss scans (NL) of 615 to profile ($PtdInsP_3$ + 7Met), 507 to profile ($PtdInsP_2$ + 5Met), 399 to profile (PtdInsP + 3Met), and 291 to profile (PtdIns + 1Met) in mice livers, when 5 mM ammonium formate was included in the LC mobile phases. The shaded areas in total ion chromatograms indicate the retention time windows where 38:5 PtdInsPs, 36:4 PtdInsPs, and 34:2 PtdInsPs (A) and 38:4 PtdInsPs (B) were eluted. 38:5 PtdInsPs, 36:4 PtdInsPs, and 38:4 PtdInsPs were assigned as 18:1/20:4 PtdInsPs, 16:0/20:4 PtdInsPs, and 18:0/20:4 PtdInsPs, respectively, after precursor ion scans were performed to identify *sn*-1 fatty acids. ND, not detected. Very similar mass spectra were obtained using cells as well (not shown).

loss scan and a precursor ion scan, specific to the structural characteristics of PtdInsPs, were performed in the positive ion mode. Collision energies of 23–46 V were used for the neutral loss scans depending on neutral loss masses, and 53 V collision energy was used for the precursor ion scans. The extracted ion chromatogram (EIC) corresponding to the specific lipid was used for relative quantitation after normalization using the internal standard. LC/MS/MS data were analyzed with Analyst 1.5.2 software (AB Sciex). Each of the 17:0/20:4 PtdIns, 17:0/20:4 PtdInsP, 17:0/20:4 $PtdInsP_2$, and 17:0/20:4 $PtdInsP_3$ were used to normalize the corresponding PtdInsPs having different numbers of phosphorylation.

RESULTS AND DISCUSSION

Ammonium adducts for PtdInsPs

PtdInsPs were permethylated via chemical derivatization with TMS-diazomethane. Incubation with TMS-diazomethane at room temperature for 30 min reproducibly formed permethylated PtdInsPs. Oxygen atoms within the phosphate hydroxyl groups were known to be methylated (35). All phosphate groups were permethylated after the reaction in our study. For example, 17:0/20:4 $PtdInsP_2$ contains five hydroxyl groups on phosphates, including a

TABLE 1. Signal enhancement due to ammonium ion adduction

	Signal Enhancement (n = 3)			
Concentration (pmol/ml)	18:0/20:4 PtdIns + 1Met	18:1/18:1 PtdInsP + 3Met	18:0/20:4 $PtdInsP_2$ + 5Met	18:0/20:4 $PtdInsP_3$ + 7Met
10	4.8	1.8	2.1	2.4
100	5.8	1.6	2.6	2.3
1,000	5.7	2.1	2.2	2.1

The signal enhancement was the peak area ratio of ammonium ion adducted PtdInsPs to protonated PtdInsPs. Peak areas of ammonium ion adducted or protonated PtdInsPs were obtained when either ammonium formate or formic acid was included in LC mobile phases.

TABLE 2. Reproducibility in the quantification of ammonium ion adducts of PtdInsPs

Concentration (pmol/ml)	Observed (n = 3) 18:0/20:4 PtdIns + 1Met		18:1/18:1 PtdInsP + 3Met		18:0/20:4 $PtdInsP_2$ + 5Met		18:0/20:4 $PtdInsP_3$ + 7Met	
Expected	Mean	(RSD)	Mean	(RSD)	Mean	(RSD)	Mean	(RSD)
10	10	(23)	10	(5)	12	(25)	12	(17)
100	128	(13)	120	(12)	109	(10)	112	(16)
1,000	1,095	(9)	1,090	(8)	1,160	(5)	1,127	(11)

Neutral loss scans were performed, and peak areas for specific PtdInsPs were used to evaluate the reproducibility of ammonium ion adduct formation. The peak area of each PtdInsPs species was normalized to that of the corresponding internal standard. RSD indicates the relative standard deviation of three experiments.

phosphate attached to the glycerol backbone; 17:0/20:4 $PtdInsP_2$ + 5Met was mainly observed, although overmethylated PtdInsPs were found as well, but at lower abundances (**Fig. 1**).

Adduct formation such as $[M + NH_4]^+$ or $[M + Na]^+$ is commonly observed in mass spectrometric analyses. Although adduct formation often enhances ionization efficiencies of analytes, these phenomena may not be reproducible and may complicate the quantitative analysis and interpretation of MS/MS spectra. We rarely observed sodium or potassium ion adduct formation for permethylated PtdInsPs. On the contrary, signal intensities of ammonium adducts with permethylated PtdInsPs were generally comparable to those of protonated forms in the positive ion mode. Figure 1A shows the mass spectrum of permethylated PtdInsPs without ammonium ion additive in the LC mobile phase. Generally, $[M + xMet + H]^+$ (M = PtdInsPs) was the most abundant ion for specific PtdInsPs species, except 17:0/20:4 PtdIns. However, as shown in Fig. 1B, $[M + xMet + NH_4]^+$ was the most abundant ion for specific PtdInsPs species than the corresponding $[M + H]^+$ when ammonium ion additive was included in the LC mobile phase, and ammonium ion additive enhanced signal intensities for PtdInsPs. Thus, ammonium ion additive was added into the LC mobile phases for signal enhancement and stable ammonium adduct formation.

Ammonium ion adduction may complicate the MS/MS spectra. Thus, we compared MS/MS spectra of $[M + NH_4]^+$ and $[M + H]^+$. The major fragment ion was DAG in CID of either $[M + NH_4]^+$ or $[M + H]^+$. As shown in **Fig. 2A**, B, *m/z* 627 corresponding to 18:0/20:4 DAG was the most abundant ion; *m/z* 341 corresponding to 18:0 MAG was also observed and formed from further cleavage occurring at the C-O bond of the *sn*-2 position. This fragmentation provided additional structural information regarding fatty acids attached at the *sn*-1 position of PtdInsPs. Similarly, the fragmentation pattern between $[M + NH_4]^+$ and $[M + H]^+$ was the same for other PtdInsPs (supplemental Fig. S1). Thus, ammonium adducts of permethylated PtdInsPs were used for quantitative structural characterization of PtdInsPs in this study.

The neutral loss scans of headgroups could observe 34:2 PtdInsPs, 16:0/20:4 PtdInsPs, 18:0/20:4 PtdInsPs, and 18:1/20:4 PtdInsPs from mice livers as shown in **Fig. 3A**, B, where 18:0/20:4 PtdInsPs were found at different retention time from 34:2 PtdInsPs, 16:0/20:4 PtdInsPs, and 18:1/20:4 PtdInsPs. The 17:0/20:4 PtdInsPs, used as internal standards, were also found at another retention time. The number of phosphorylations of inositol phosphates did not affect the LC elution time among PtdInsPs with the same fatty acyl compositions. Fewer PtdInsPs species were observed when ammonium ion additive was not included in the LC mobile phases (supplemental Fig. S2). When the same PtdInsPs were observed, the signal enhancement due to ammonium ion adduction ranged between 2- and 10-fold depending on PtdInsPs species.

The benefit of addition of ammonium ion in mobile phases for signal enhancement and reproducible analysis was demonstrated by several groups using small chemicals (37, 38). We wanted to identify PtdInsPs from biological samples such as cells and mice livers, and also to obtain the relative quantitation of PtdInsPs. Reproducibility and signal enhancement of ammonium ion adducted PtdInsPs were evaluated from three independent experiments. Signal enhancement due to ammonium ion adduction was evaluated using peak areas of ammonium ion-adducted PtdInsPs to protonated PtdInsPs in **Table 1**. Generally, 2- to 6-fold signal enhancement was expected due to ammonium ion adduction. Reproducible ammonium ion adduct formation of PtdInsPs was evaluated, and the relative standard deviation for each type of PtdInsPs was shown in **Table 2**. Linearity of neutral loss scans of each PtdInsP was evaluated as shown in supplemental Fig. S3. Ammonium ion adduct formation of PtdInsPs was stable and reproducible, and neutral loss scans provided a linear relationship between signal responses and amounts of PtdInsPs. Precursor ion scans also enabled reproducible quantitation of PtdInsPs; however, the ion abundances of precursor ion scans of *sn*-1 MAG were lower than neutral loss scans of headgroups. Thus, we used neutral loss scans for relative quantitation of PtdInsPs from biological samples.

Structural identification of *sn*-1 and *sn*-2 fatty acids of PtdInsPs

Permethylated PtdInsPs provided DAGs as major fragment ions in CID spectra as shown in the previous section. Thus, neutral loss scans, corresponding to phosphoinositol headgroups, have been performed to profile PtdInsPs. Clark et al. (35) also used a similar strategy to profile PtdInsPs, and they used a neutral loss scan of 598 to profile $PtdInsP_3$. In the present study, a neutral loss scan of 615 was used to profile potential $PtdInsP_3$ isomers due to ammonium

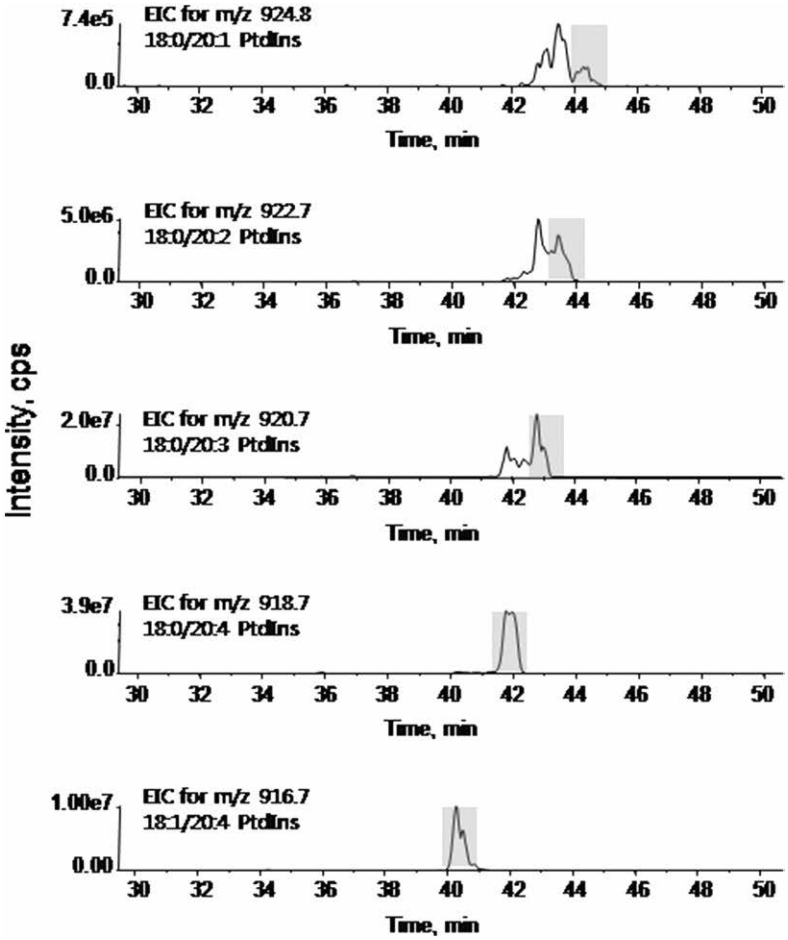

Fig. 4. EICs from neutral loss scans of 291 to profile $[PtdIns + 1Met + NH_4]^+$ in insulin-treated cells, when 5 mM ammonium formate was included in the LC mobile phases. The shaded area in each EIC indicates the retention time window, where 38:1 PtdIns, 38:2 PtdIns, 38:3 PtdIns, 38:4 PtdIns, or 38:5 PtdIns was eluted. Each PtdIns was assigned as 18:0/20:1 PtdIns, 18:0/20:2 PtdIns, 18:0/20:3 PtdIns, 18:0/20:4 PtdIns, or 18:1/20:5 PtdIns, respectively, after precursor ion scans were performed to identify *sn*-1 fatty acids.

ion adduction. Likewise, neutral loss scans of 507, 399, and 291 were used to profile $PtdInsP_2$, PtdInsP, and PtdIns species, respectively, from cells and mice livers.

A neutral loss scan only provides the number of phosphate groups in the inositol phosphates of PtdInsPs, but fatty acyl compositions at the *sn*-1 and *sn*-2 positions could not be identified. CID spectra for PtdInsPs should be obtained to confirm the complete structural characterization of the lipid species (35). Potential PtdInsPs in biological samples should be selected from a neutral loss scan result for complete structural elucidation of the PtdInsPs, and this process is often complicated and tedious. Then, MS^2 experiments for all potential PtdInsPs should be performed with frequent modification of the method depending on specific PtdInsPs observed in biological samples. Otherwise, the composition of fatty acyl chains in PtdInsPs could not be identified only with the neutral loss scan result. For example, *m/z* 1,134.6 from a neutral loss scan of 507 would be identified as 38:4 $PtdInsP_2$, but its fatty acyl composition could be any of the following molecular species: 16:0/22:4 $PtdInsP_2$, 18:0/20:4 $PtdInsP_2$, 18:1/20:3 $PtdInsP_2$, or other possibilities. DAG-specific precursor ion scans could not elucidate the fatty acyl compositions at the *sn*-1 and *sn*-2 positions of PtdInsPs either (39).

In our present study, precursor ion scans of *sn*-1 MAG were performed to identify *sn*-1 fatty acid of PtdInsPs in positive ion mode. Mass differences of 108 Da among differentially phosphorylated PtdInsPs having the same fatty acyl compositions and comparison of LC retention times from neutral scan spectra enabled us identify the unknown PtdInsPs with *sn*-1 fatty acid information. Biological samples were known to primarily contain 16:0, 18:1, and 18:0 fatty acids at the *sn*-1 position of phospholipids (40). Thus, we included precursor ion scans for 16:0, 18:1, and 18:0 fatty acids, as well as 17:0 for internal standards, and the precursor ion scan could then be modified depending on the fatty acid compositions of any PtdInsPs.

The neutral loss scans for insulin-treated AML12 cells could observe 18:1/20:4 PtdInsPs, 18:0/20:4 PtdInsPs, 18:0/20:3 PtdInsPs, 16:0/20:4 PtdInsPs, 16:0/20:3 PtdInsPs, and so forth. The EICs generated from the neutral loss scan of 291 for PtdIns are shown in **Fig. 4**. The *sn*-1 and *sn*-2 fatty acids of PtdIns were assigned with specific fatty acid compositions using the result from precursor ion scans shown in **Fig. 5**. PtdInsPs having fewer unsaturated fatty acids or longer chain fatty acids were likely to elute late as shown in Fig. 3 and Fig. 4. Precursor ion scan of 341 was performed to find PtdInsPs having stearic acid at the *sn*-1 position shown in Fig. 5, where mass spectra were generated for the shaded retention time areas. EIC for *m/z* 920.7 from neutral loss scan of 291 shows two peaks in Fig. 4. The peak eluted later (42.5–43.5 min) should come from 18:0/20:3 PtdIns, which is confirmed from Fig. 5B. However, the peak eluted earlier (41.5–42.5 min) might not be any PtdIns species or might be generated from the second isotope of 18:0/20:4 PtdIns, as assumed from Fig. 5A. For that retention time, 18:0/20/4

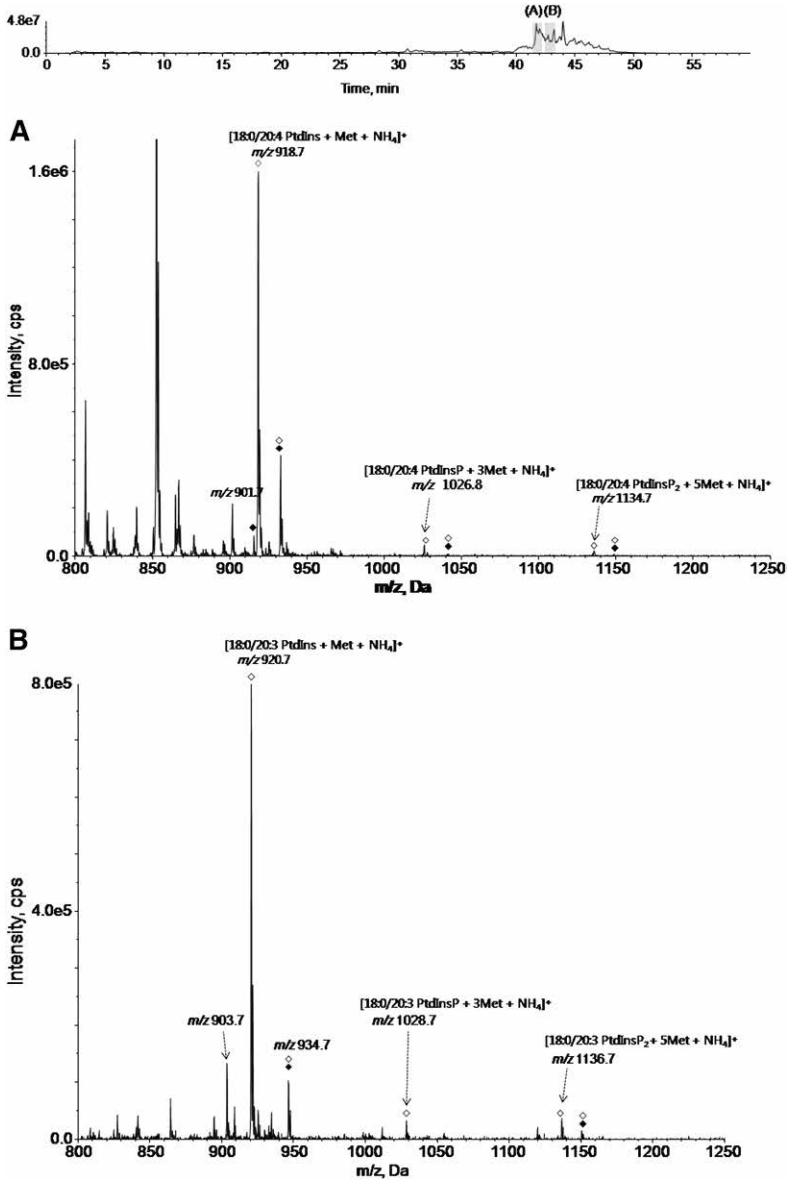

Fig. 5. Mass spectra of precursor ion scans of 341 to profile PtdInsPs containing 18:0 fatty acids at *sn*-1 position of glycerol backbone from insulin-treated cells, when 5 mM ammonium formate was included in the LC mobile phases. The shaded areas in the chromatograms indicate the retention time windows where 18:0/20:4 PtdInsPs (A) and 18:0/20:3 PtdInsPs (B) were eluted. The number of filled diamonds indicates the number of overmethylation to each permethylated PtdInsP, and open diamonds indicate ammonium ion adduction.

PtdInsPs were the only PtdInsPs molecular species observable; thus the peak eluted at 41.5–42.5 min was assigned as 18:0/20:4 PtdIns. Likewise, shaded peaks for *m/z* 922.7 and *m/z* 924.8 were assigned as 18:0/20:2 PtdIns and 18:0/20:1 PtdIns, respectively. Precursor ion scans also enabled reproducible quantitation of PtdInsPs; however, the ion abundances of precursor ion scans of *sn*-1 MAG were lower than neutral loss scans of headgroups in positive ion mode. Thus, we used neutral loss scans for relative quantitation of PtdInsPs from biological samples. $PtdInsP_3$'s were observed only from neutral loss scan analysis, and their *sn*-1 fatty acyl compositions were assigned when fewer phosphorylated $PtdInsP_2$ and PtdInsP species with the same fatty acyl compositions were observed at the same retention time, as shown in Fig. 5A and supplemental Fig. S4.

Quantitative profiling of PtdInsPs

Insulin has been shown to stimulate Akt phosphorylation via activation of PI3K (41). Western blot analysis shows Akt phosphorylation by insulin as shown in **Fig. 6A**, and highly phosphorylated PtdInsPs were expected to be increased. Changes of PtdInsPs in AML12 cells after insulin stimulation are shown in Fig. 6B. $PtdInsP_3$ was increased after insulin treatment, compared with the corresponding $PtdInsP_3$ from control cells. The ion abundances of precursor ion scans of *sn*-1 MAG were lower than neutral loss scans of phosphoinositol headgroups. Thus, we used neutral loss scans for the quantitation of PtdInsPs from biological samples. EIC for each species of 18:0/20:4 PtdInsPs from neutral scan analysis are shown in supplemental Fig. S4, and the peak area of all PtdInsPs observed are shown in supplemental Table S1A.

Changes of PtdInsPs in insulin-stimulated mice livers are shown in **Fig. 7**. Peak areas of all PtdInsPs observed are shown in supplemental Table S1B. Highly phosphorylated 18:0/20:4 $PtdInsP_3$ were increased the most for insulin stimulation, compared with the corresponding $PtdInsP_3$ from control livers. Generally, PtdInsP expression in livers

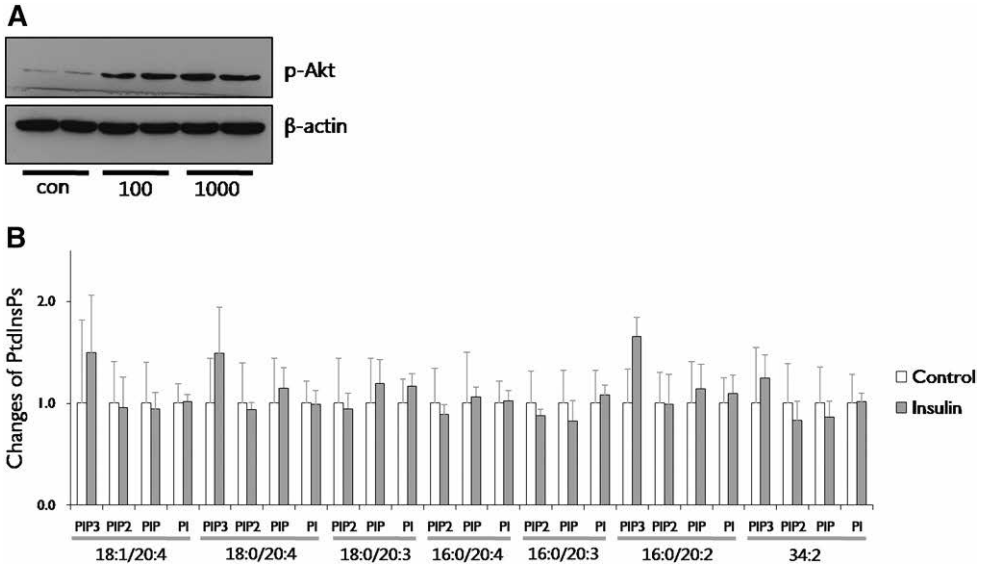

Fig. 6. (A) Western blot analysis of extracts from insulin-treated cells. "Con" means AML12 cells without insulin treatment; 100 or 1,000 indicates either 100 ng/ml or 1,000 ng/ml of insulin-treated AML12 cells. (B) Changes of PtdInsPs after 20 min incubation with 100 ng/ml of insulin. The 1,000 ng/ml of insulin-treated cells shows a similar result; data not shown. Peak area was the normalized peak area of each PtdInsPs to the corresponding internal standard from neutral loss scan analysis. Changes of PtdInsPs were calculated by dividing the average peak areas of PtdInsPs in insulin-stimulated cells by those in control cells. Error bars indicate the relative standard deviations of independently prepared samples (n = 3). Neutral loss scans of headgroups were used for quantitation, and EICs for specific PtdInsPs can be found in Fig. 4 and supplemental Fig. S4.

was increased after insulin treatment, but PtdIns expression was decreased. Interestingly, $PtdInsP_2$ levels in cells and livers were not increased when the $PtdInsP_3$ increment was obvious after insulin stimulation. The major fatty acyl composition of PtdInsPs in mice livers was 18:0/20:4 PtdInsPs, and the amount of 18:0/20:4 PtdInsPs constitutes ~80%–90% of all observed PtdInsPs.

CONCLUSION

Our result shows that the combined strategy of the neutral loss scans of phosphoinositol headgroups and precursor ion scans of *sn*-1 MAG is able to profile quantitatively PtdInsPs with structural information of the *sn*-1 and *sn*-2 fatty acids, and stable ammonium ion adduction is especially beneficial to observe more PtdInsPs. Quantitative profiling of PtdInsPs in cells and tissues was successfully performed with structural information of the *sn*-1 and *sn*-2 fatty acid compositions. $PtdInsP_3$'s were observed only for some of PtdInsPs in the samples we used. Although major fatty acid compositions of PtdInsPs were 18:0/20:4 PtdInsPs for hepatocytes and livers, these fatty acid compositions might vary depending on the types of cells and tissues. Regioisomers of PtdInsPs, considering different phosphorylation sites on the inositol groups, could not be resolved with this method, and solving this problem remains part of our future work.

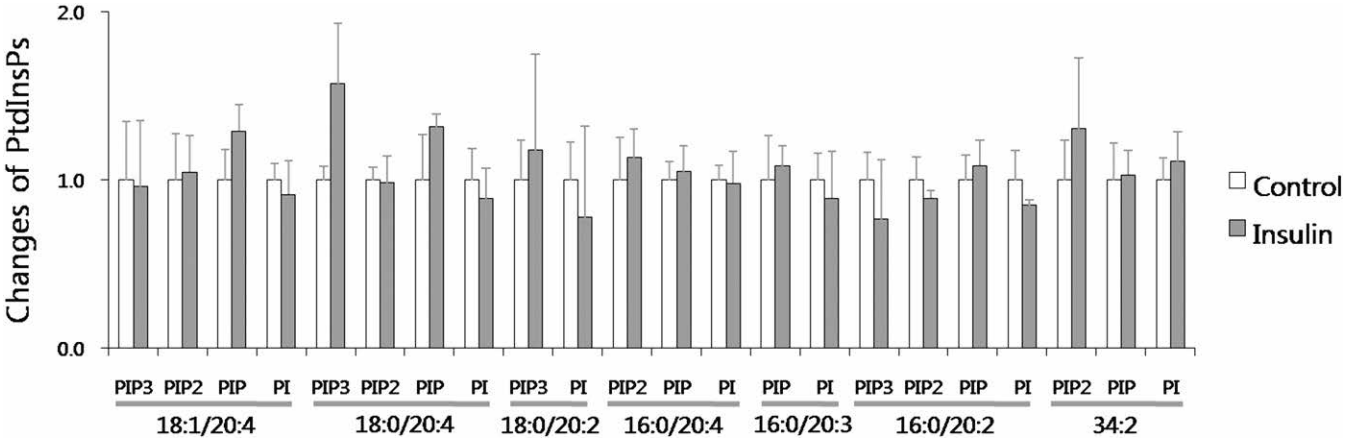

Fig. 7. Changes of PtdInsPs in insulin-stimulated mice livers. Changes of PtdInsPs were calculated by dividing the average peak areas of PtdInsPs in insulin-stimulated mice livers by those in control livers. Error bars indicate the relative standard deviations of independently prepared samples (n = 4).

REFERENCES

1. Toker, A. 2002. Phosphoinositides and signal transduction. *Cell. Mol. Life Sci.* **59:** 761–779.
2. Mayinger, P. 2012. Phosphoinositides and vesicular membrane traffic. *Biochim. Biophys. Acta.* **1821:** 1104–1113.
3. Okada, M., S. W. Jang, and K. Ye. 2008. Akt phosphorylation and nuclear phosphoinositide association mediate mRNA export and cell proliferation activities by ALY. *Proc. Natl. Acad. Sci. USA.* **105:** 8649–8654.
4. Rajala, R. V., A. Rajala, A. J. Morris, and R. E. Anderson. 2014. Phosphoinositides: minor lipids make a major impact on photoreceptor cell functions. *Sci. Rep.* **4:** 5463.
5. Vivanco, I., and C. L. Sawyers. 2002. The phosphatidylinositol 3-kinase AKT pathway in human cancer. *Nat. Rev. Cancer.* **2:** 489–501.
6. Kim, I., H. G. Kim, J. N. So, J. H. Kim, H. J. Kwak, and G. Y. Koh. 2000. Angiopoietin-1 regulates endothelial cell survival through the phosphatidylinositol 3′-kinase/Akt signal transduction pathway. *Circ. Res.* **86:** 24–29.
7. Di Paolo, G., and P. De Camilli. 2006. Phosphoinositides in cell regulation and membrane dynamics. *Nature.* **443:** 651–657.
8. Krauss, M., and V. Haucke. 2007. Phosphoinositide-metabolizing enzymes at the interface between membrane traffic and cell signalling. *EMBO Rep.* **8:** 241–246.
9. Engelman, J. A., J. Luo, and L. C. Cantley. 2006. The evolution of phosphatidylinositol 3-kinases as regulators of growth and metabolism. *Nat. Rev. Genet.* **7:** 606–619.
10. Balla, T. 2013. Phosphoinositides: tiny lipids with giant impact on cell regulation. *Physiol. Rev.* **93:** 1019–1137.
11. Manna, P., and S. K. Jain. 2015. Phosphatidylinositol-3,4,5-triphosphate and cellular signaling: implications for obesity and diabetes. *Cell. Physiol. Biochem.* **35:** 1253–1275.
12. Nasuhoglu, C., S. Feng, J. Mao, M. Yamamoto, H. L. Yin, S. Earnest, B. Barylko, J. P. Albanesi, and D. W. Hilgemann. 2002. Nonradioactive analysis of phosphatidylinositides and other anionic phospholipids by anion-exchange high-performance liquid chromatography with suppressed conductivity detection. *Anal. Biochem.* **301:** 243–254.
13. Wenk, M. R., L. Lucast, G. Di Paolo, A. J. Romanelli, S. F. Suchy, R. L. Nussbaum, G. W. Cline, G. I. Shulman, W. McMurray, and P. De Camilli. 2003. Phosphoinositide profiling in complex lipid mixtures using electrospray ionization mass spectrometry. *Nat. Biotechnol.* **21:** 813–817.
14. Kielkowska, A., I. Niewczas, K. E. Anderson, T. N. Durrant, J. Clark, L. R. Stephens, and P. T. Hawkins. 2014. A new approach to measuring phosphoinositides in cells by mass spectrometry. *Adv. Biol. Regul.* **54:** 131–141.
15. Stephens, L. R., T. R. Jackson, and P. T. Hawkins. 1993. Agonist-stimulated synthesis of phosphatidylinositol(3,4,5)-trisphosphate: a new intracellular signalling system? *Biochim. Biophys. Acta.* **1179:** 27–75.
16. Milne, S. B., P. T. Ivanova, D. DeCamp, R. C. Hsueh, and H. A. Brown. 2005. A targeted mass spectrometric analysis of phosphatidylinositol phosphate species. *J. Lipid Res.* **46:** 1796–1802.
17. Haag, M., A. Schmidt, T. Sachsenheimer, and B. Brugger. 2012. Quantification of signaling lipids by nano-electrospray ionization tandem mass spectrometry (nano-ESI MS/MS). *Metabolites.* **2:** 57–76.
18. Alter, C. A., and B. A. Wolf. 1995. Identification of phosphatidylinositol 3,4,5-trisphosphate in pancreatic islets and insulin-secreting beta-cells. *Biochem. Biophys. Res. Commun.* **208:** 190–197.
19. Ho, C. Y., C. H. Choy, and R. J. Botelho. 2016. Radiolabeling and quantification of cellular levels of phosphoinositides by high performance liquid chromatography-coupled flow scintillation. *J. Vis. Exp.* **107:** e53529.
20. Hama, H., J. Torabinejad, G. D. Prestwich, and D. B. DeWald. 2004. Measurement and immunofluorescence of cellular phosphoinositides. *Methods Mol. Biol.* **284:** 243–258.
21. Hegewald, H. 1996. One-dimensional thin-layer chromatography of all known D-3 and D-4 isomers of phosphoinositides. *Anal. Biochem.* **242:** 152–155.
22. Furutani, M., T. Itoh, T. Ijuin, K. Tsujita, and T. Takenawa. 2006. Thin layer chromatography-blotting, a novel method for the detection of phosphoinositides. *J. Biochem.* **139:** 663–670.
23. König, S., M. Hoffmann, A. Mosblech, and I. Heilmann. 2008. Determination of content and fatty acid composition of unlabeled phosphoinositide species by thin-layer chromatography and gas chromatography. *Anal. Biochem.* **378:** 197–201.
24. Michelsen, P., B. Jergil, and G. Odham. 1995. Quantification of polyphosphoinositides using selected ion monitoring electrospray mass spectrometry. *Rapid Commun. Mass Spectrom.* **9:** 1109–1114.
25. Hsu, F. F., and J. Turk. 2000. Characterization of phosphatidylinositol, phosphatidylinositol-4-phosphate, and phosphatidylinositol-4,5-bisphosphate by electrospray ionization tandem mass spectrometry: a mechanistic study. *J. Am. Soc. Mass Spectrom.* **11:** 986–999.
26. Van Beveren, C., F. van Straaten, J. A. Galleshaw, and I. M. Verma. 1981. Nucleotide sequence of the genome of a murine sarcoma virus. *Cell.* **27:** 97–108.
27. Gross, C., C. W. Chang, S. M. Kelly, A. Bhattacharya, S. M. McBride, S. W. Danielson, M. Q. Jiang, C. B. Chan, K. Ye, J. R. Gibson, et al. 2015. Increased expression of the PI3K enhancer PIKE mediates deficits in synaptic plasticity and behavior in fragile X syndrome. Cell Rep. 11:727–736.
28. Pettitt, T. R. 2010. Phosphoinositide analysis by liquid chromatography-mass spectrometry. *Methods Mol. Biol.* **645:** 203–217.
29. Pettus, B. J., C. E. Chalfant, and Y. A. Hannun. 2002. Ceramide in apoptosis: an overview and current perspectives. *Biochim. Biophys. Acta.* **1585:** 114–125.
30. Ogiso, H., and R. Taguchi. 2008. Reversed-phase LC/MS method for polyphosphoinositide analyses: changes in molecular species levels during epidermal growth factor activation in A431 cells. *Anal. Chem.* **80:** 9226–9232.
31. Pettitt, T. R., S. K. Dove, A. Lubben, S. D. Calaminus, and M. J. Wakelam. 2006. Analysis of intact phosphoinositides in biological samples. *J. Lipid Res.* **47:** 1588–1596.
32. Kühnel, E., D. D. Laffan, G. C. Lloyd-Jones, T. Martínez Del Campo, I. R. Shepperson, and J. L. Slaughter. 2007. Mechanism of methyl esterification of carboxylic acids by trimethylsilyldiazomethane. *Angew. Chem. Int. Ed. Engl.* **46:** 7075–7078.
33. Wasslen, K. V., C. R. Canez, H. Lee, J. M. Manthorpe, and J. C. Smith. 2014. Trimethylation enhancement using diazomethane (TrEnDi) II: rapid in-solution concomitant quaternization of glycerophospholipid amino groups and methylation of phosphate groups via reaction with diazomethane significantly enhances sensitivity in mass spectrometry analyses via a fixed, permanent positive charge. *Anal. Chem.* **86:** 9523–9532.
34. Lee, J. W., S. Nishiumi, M. Yoshida, E. Fukusaki, and T. Bamba. 2013. Simultaneous profiling of polar lipids by supercritical fluid chromatography/tandem mass spectrometry with methylation. *J. Chromatogr. A.* **1279:** 98–107.
35. Clark, J., K. E. Anderson, V. Juvin, T. S. Smith, F. Karpe, M. J. Wakelam, L. R. Stephens, and P. T. Hawkins. 2011. Quantification of PtdInsP3 molecular species in cells and tissues by mass spectrometry. *Nat. Methods.* **8:** 267–272.
36. Bligh, E. G., and W. J. Dyer. 1959. A rapid method of total lipid extraction and purification. *Can. J. Biochem. Physiol.* **37:** 911–917.
37. Lim, C. W., S. H. Tai, L. M. Lee, and S. H. Chan. 2012. Analytical method for the accurate determination of tricothecenes in grains using LC-MS/MS: a comparison between MRM transition and MS3 quantitation. *Anal. Bioanal. Chem.* **403:** 2801–2806.
38. Mortier, K. A., G. Zhang, C. H. V. Peteghem, and W. E. Lamber. 2004. Adduct formation of quantitative bioanalysis: Effect of ionization conditions on paclitaxel. *J. Am. Soc. Mass Spectrom.* **15:** 585–592.
39. Cai, T., Q. Shu, J. Hou, P. Liu, L. Niu, X. Guo, C. C. Liu, and F. Yang. 2015. Profiling and relative quantitation of phosphoinositides by multiple precursor ion scanning based on phosphate methylation and isotopic labeling. *Anal. Chem.* **87:** 513–521.
40. Geyer, R. P., Bennett, A., and A. Rohr. 1962. Fatty acids of the triglycerides and phospholipids of HeLa cells and strain L fibroblasts. *J. Lipid Res.* **3:** 80–83.
41. Hermann, C., B. Assmus, C. Urbich, A. M. Zeiher, and S. Dimmeler. 2000. Insulin-mediated stimulation of protein kinase Akt: a potent survival signaling cascade for endothelial cells. *Arterioscler. Thromb. Vasc. Biol.* **20:** 402–409.